TLS BOOSTER INJECTION SCHEME EXPLORATION*

Hsin-Hui Chen†, Ho-Ping Chang, Hung-Chiao Chen, Yao-Kwang Lin, Jar-An Li, Szu-Jung Huang, Changhor Kuo, An-ping Lee, Ke-Kang Lin, NSRRC, Hsinchu, Taiwan

Abstract

In this paper, the booster injection efficiency and the parameter working range related to key components including septum magnet and kicker magnet for Taiwan Light Source (TLS) injector operation are introduced. Booster injection scheme for different lattice is explored by machine study plan using injector property. The study result may be used by the operator as booster injection parameter fine tuning reference. It is also helpful for the advanced injection scheme exploration.

INTRODUCTION

TLS pre-injector is turnkey system made by Sweden Scanditronix Company. It contains hot cathode electron gun (e-gun), linear accelerator (LINAC) and bending transport line (see Fig. 1). Pre-injector accelerates the electrons gun emitted from energy 140 KeV to 50 MeV, then injects electrons into booster thru 60 degree bend-ing transport line. The pre-injector scheme is electrons pass septum magnet into one FODO cell (QD-BEND-QD), then on-axis injected by kicker magnet to 72 meters circumference booster (see Fig. 2).

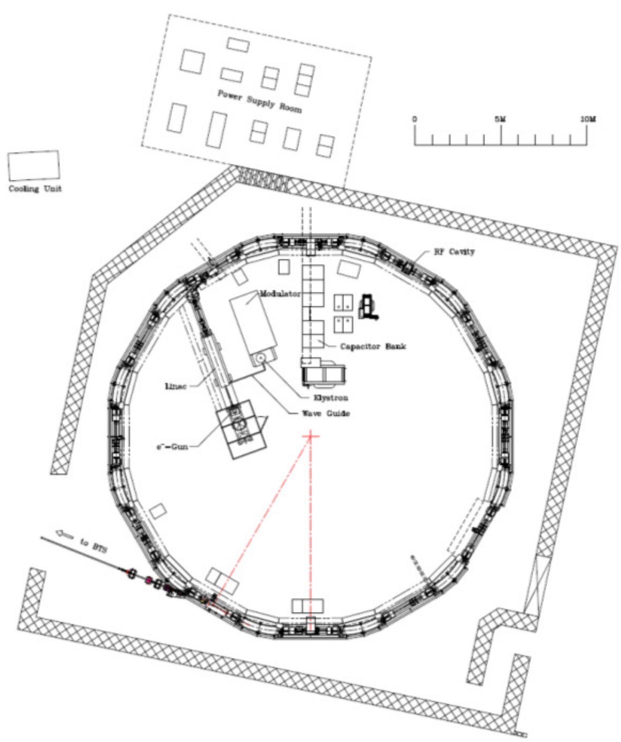

Figure 1: TLS pre-injector and booster.

The phase-space chart [1] of booster injector scheme shows the function of each magnet. The septum and kicker magnets are on the first and last position of transport line. They are the key components related to high injection efficiency with low radiation (see Fig. 3).

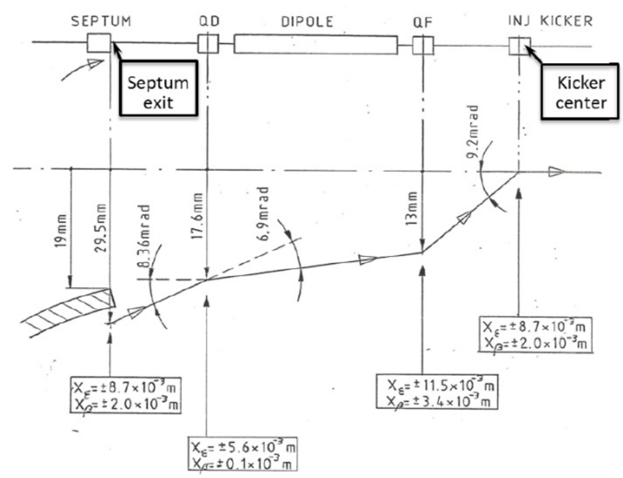

Figure 2: Scheme of TLS pre-injector and transport line.

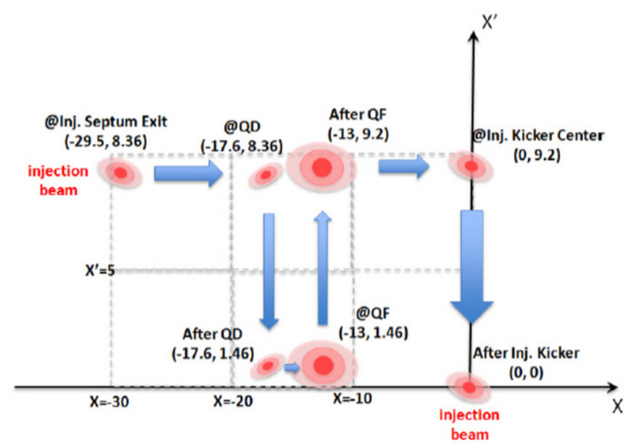

Figure 3: Phase-space chart of booster injector scheme.

DYNAMIC APERTURE

The dynamic aperture at kicker magnet can be calculated by measuring septum magnet voltages with kicker magnet modulation. The pre-injector magnet length and position data is in Table 1 for electron phase-space chart calculation. All these measurements are well controlled with same booster lattice for operation.

Phase Space Chart Calculation

The electron beam exit position from septum magnet and entrance angle into kicker magnet are calculated by booster current with modulated septum magnet voltage. Then data is converted to electron beam position and angle at the kicker magnet.

The phase-space chart of electron beam with respect to axis center of kicker magnet is calculated. The x and y-

* Work supported by National Synchrotron Radiation Research Center
† chen.owen@nsrrc.org.tw

axis shows the electron beam position and angle with respect to injection kicker center axis (see Fig. 4).

Table 1: Magnet length and position data

Element	Length(m)	Position(m)
Injection septum exit	0	0
LSS	1.02	1.02
SD	0.1	1.12
QSSS	0.15	1.27
QD-1/2	0.15	1.42
QD-center	0	1.42
QD-1/2	0.15	1.57
QDSS	0.23	1.8
DIP	2.4	4.2
QDSS	0.23	4.43
QF-1/2	0.15	4.58
QF-center	0	4.58
QF-1/2	0.15	4.73
QSSS	0.15	4.88
SF	0.1	4.98
LSS	1.02	6
Kicker-center	0	6

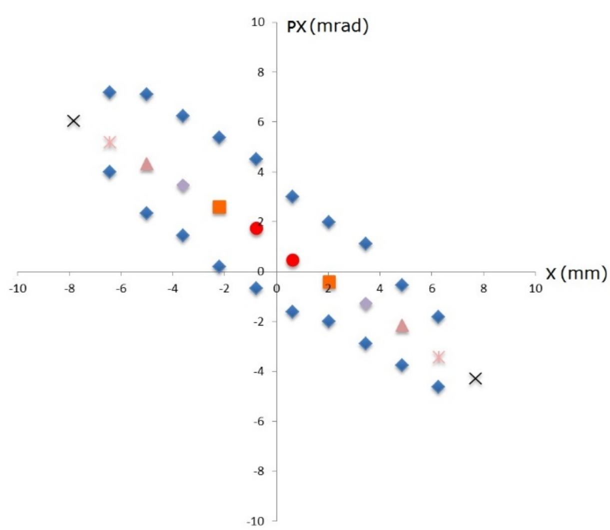

Figure 4: Calculated electron beam phase-space chart.

The controlled booster lattice keep the same electron beam condition at entrance of septum magnet. Electron beam position and angle at kicker magnet changes with different septum voltage thru FODO cell. The calculated phase-space chart shows the beam position and angle at kicker magnet varies with modulated septum magnet voltage (boundary and center values).

Aperture Boundary

The phase-space chart shows the boundary and optimal working points. The black dot line is the boundary value with no booster current. The injection efficiency with boundary condition is zero. The green dot line is the optimal value with best injection efficiency (see Fig. 5).

The optimal value green line doesn't cross the origin point as estimation for the booster closed orbit distortion. This distortion was produced by assembly and installation error. The magnet field error also contributes the distortion. No corrector magnet is implemented for closed orbit distortion on booster. Measured beam dynamic aperture is smaller than the modelling for electron boosting interference.

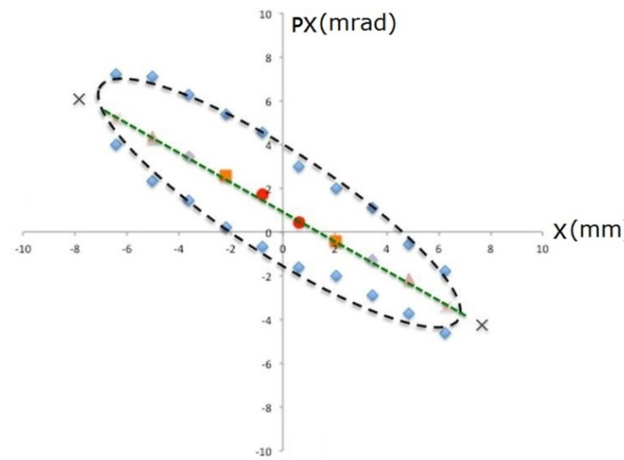

Figure 5: Measured beam phase-space boundary and optimal working points.

Injection Efficiency

The dynamic aperture shows the injection efficiency with concentric ovals. Injection efficiency decreases from inner to outer ovals (see Fig. 6). The optimal booster current measurement also shows the same trend with dynamic aperture (see Fig. 7).

Electron beam phase-space point moves toward 4th quadrant with positive modulation of septum magnet voltage. Septum magnet voltage increasing gets higher injection efficiency. Beam phase-space point moves toward 2nd quadrant with negative modulation of septum magnet voltage. Kicker magnet voltage decreasing also gets the higher injection efficiency.

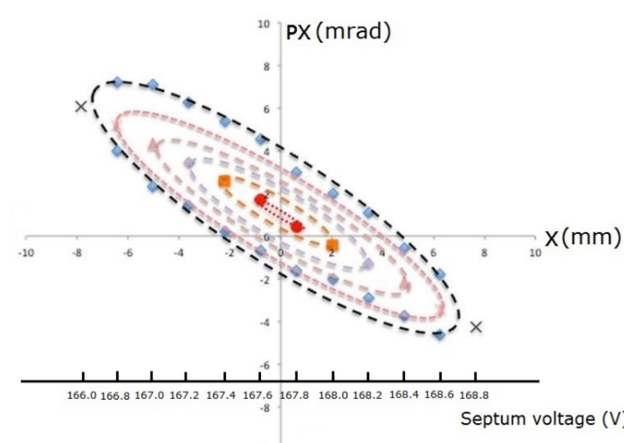

Figure 6: Measured dynamic aperture injection efficiency concentric ovals.

ISBN 978-3-95450-147-2

The beam injected position and angle data at kicker magnet are listed in Table 2. The nominal values of beam injected position and angle are displayed as best injection efficiency (green dot line) as Figure 5. The beam injected position and angle data is calculated with tested septum magnet voltage.

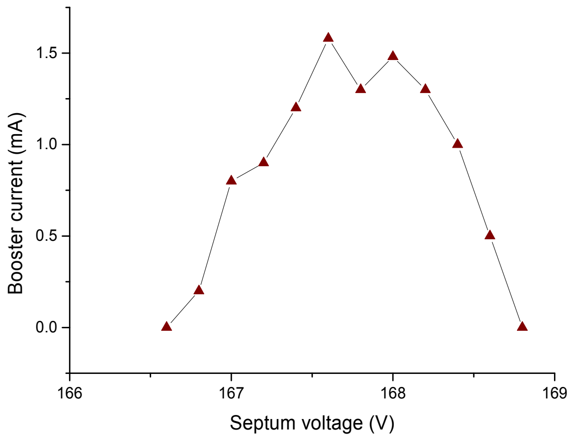

Figure 7: Measured optimal booster current with different septum magnet voltages.

Table 2: Beam injected position and angle at kicker magnet (nominal value)

Septum(V)	Kicker-X(mm)	Kicker-PX(mrad)
166.60	7.682	-4.281
166.80	6.271	-3.415
167.00	4.859	-2.148
167.20	3.448	-1.281
167.40	2.036	-0.414
167.60	0.625	0.456
167.80	-0.785	1.718
168.00	-2.197	2.586
168.20	-3.608	3.454
168.40	-5.020	4.322
168.60	-6.431	5.187
168.80	-7.843	6.052

CONCLUSION

The analysis between real operation and theoretical calculation can be implemented on operation parameter tuning. The kicker magnet voltage can compensate septum magnet voltage bias. Working characteristics of septum and kicker magnets are explored for operation.

REFERENCES

[1] H.P.Chang, K.L.Tsai, C.S.Fann, C.L.Chen, K.K.Lin, Introduction of the Accelerator Lattice Cells and the Study of TLS Booster Lattice by Using MAD-X, NSRRC technical report, NSRRC-Linac-2015-01, June 16, 2015.

[2] TLS booster design handbook.